

# MICROSTRUCTURES AND PROPERTIES OF MOLYBDENUM WIRES DOPED WITH La<sup>①</sup>

Zhou, Meiling\* Li, Jun\*\* Zuo, Tiejong\*\*\*

\* Department of Materials Science and Engineering,  
Beijing Polytechnic University, Beijing 100022

\*\* University of Science and Technology Beijing, Beijing 100083

\*\*\* Central South University of Technology, Changsha 410083

## ABSTRACT

The structures and properties of the La-doped molybdenum(La-Mo) powder, compact, rods and wires annealed at different temperatures were investigated. The experimental results show that the La exists in the powders in the forms of lanthanum nitrate, lanthana and complex oxides of molybdenum and lanthanum, whereas the La exists in the compacts, rods and annealed wires in the form of lanthana. Upon annealing at 1600 °C, the elongated La<sub>2</sub>O<sub>3</sub> in wires breaks up into rows of La<sub>2</sub>O<sub>3</sub> particles. The recrystallization temperature of molybdenum wires has been increased, and its ductility and the creep-resistant properties have also been improved by addition of lower-content of La<sub>2</sub>O<sub>3</sub>. Moreover, grain structure with large aspect ratio has been formed in the Mo wires doped with lower content of La<sub>2</sub>O<sub>3</sub>. When the La<sub>2</sub>O<sub>3</sub> reaches higher content, the La-Mo wires show excellent thermionic electron properties and less recrystallised low-temperature embrittlement.

**Key words:** molybdenum La microstructure recrystallization strengthening toughening

## 1 INTRODUCTION

In the earlier 1950's, there were some reports about research work on rare earth-tungsten(molybdenum) alloy. In 1970's, more interests were concentrated on rare earth-W or Mo due to the development of CeO<sub>2</sub>-W material which replaced the radioactive ThO<sub>2</sub>-W cathode in some fields. Compared to W, Mo has many advantages such as more rich natural resources, less density and much better processing property. And rare earth-Mo alloy shows much better toughness than that of rare earth-W alloy. The refining effect of Sc on Mo was reported by Lee *et al* [1]. The recrystallization temperature of Mo is increased for addition of rare earth elements[2, 3], and high temperature creep-resistant property of Mo is also improved[3].

Moreover, some research work indicates that La-Mo alloy has thermionic electron-emission capacity which reaches that of Th-W alloy[4, 5]. It is necessary to do more research work about the La-Mo alloy because it can be used not only as a structural material but also as a new type promising electron emitting material.

## 2 EXPERIMENTAL

The purity of La<sub>2</sub>O<sub>3</sub> is 99.91%. The molybdenum powders are doped with 0.2 wt.-% La<sub>2</sub>O<sub>3</sub> (LLM) and 4.0 wt.-% La<sub>2</sub>O<sub>3</sub> (HLM) as aqueous solution of La(NO<sub>3</sub>)<sub>3</sub>, respectively, and the doped Mo powders are treated in hydrogen. The particle size of La-Mo powders are measured on Fisher sieve sizer. These La-Mo powders are pressed into

① Financially supported by China Scaling Plan A under Contract No. 85-04-13; received Feb. 13, 1994

green blanks and sintered in hydrogen. Then the ingots are swaged and drawn into wires with different diameters. The La-Mo wires of  $d0.60\text{mm}$  and pure Mo wires of  $d0.65\text{mm}$  are annealed in temperature range from  $700\sim 2100\text{ }^\circ\text{C}$ . After that the resistivity and mechanical properties of annealed wires were tested, and their structures are also analysed using optical microscope, SEM and EDAX. The La-Mo powders, ingots and wires are also analysed by a D500 X-ray diffractometer.

### 3 RESULTS AND DISCUSSION

#### 3.1 Particle Size of Powder and Density of Ingot

The F. S. S. S values of PM, LLM and HLM powders are  $2.6, 2.0$  and  $3.0\mu\text{m}$ , respectively. It is clear that the Mo powders become finer by addition of small amount of  $\text{La}_2\text{O}_3$ . The densities of various Mo ingots are listed in Table 1. It can be seen that the densification of LLM and HLM is higher than that of PM due to the active sintering effect of  $\text{La}_2\text{O}_3$ . Moreover, the ingots of La-Mo have much finer grains than PM ingot ( $1730/\text{mm}^2$  for PM;  $17500/\text{mm}^2$  for HLM measured on ASTM) because of the inhibition of  $\text{La}_2\text{O}_3$  particles to the grain growth of molybdenum ingot.

Table 1 Densities of La-Mo and PM ingots

ingots	tested D. / $\text{g}\cdot\text{cm}^{-3}$	theoretical D. / $\text{g}\cdot\text{cm}^{-3}$	densification (%)
fused HLM	9.70	10.00	97.0
sintered HLM	9.57	10.00	95.7
fused LLM	9.90	10.22	96.7
fused PM	9.56	10.22	93.5

#### 3.2 Changes of La of HLM in Deformation Process

X-ray spectrum revealed that La exists in Mo powders in the forms of lanthanum nitrate and oxides of La and Mo (mainly  $\text{La}_2\text{MoO}_5$ ) when decomposed at  $350\text{ }^\circ\text{C}$ , but when this Mo powder is treated again at  $840\text{ }^\circ\text{C}$ , additional  $\text{La}_2\text{O}_3$  appeared in the Mo powder, as shown in Figs. 1(a), (b). In the blank presintered at  $1100\text{ }^\circ\text{C}$ , no lanthanum ni-

trate appeared, and La existed mainly in the form of  $\text{La}_2\text{O}_3$ , but small amount of oxides of La, Mo ( $\text{La}_2\text{MoO}_5, \text{La}_2\text{MoO}_7$ ) remained unchanged, as seen from Fig. 1(c). On the other hand, La existed in the unique form of  $\text{La}_2\text{O}_3$  in directly electric-sintered ingots, which remained unchanged in the process of swaging and drawing deformation. The shape of  $\text{La}_2\text{O}_3$ , however, undergoes some changes during swaging and drawing. In ingots, the  $\text{La}_2\text{O}_3$  particles are spherical and distribute at grain boundaries of Mo. During swaging and drawing process,  $\text{La}_2\text{O}_3$  produced plastic deformation, thus becoming elongated along the working direction, as shown in Fig. 2.

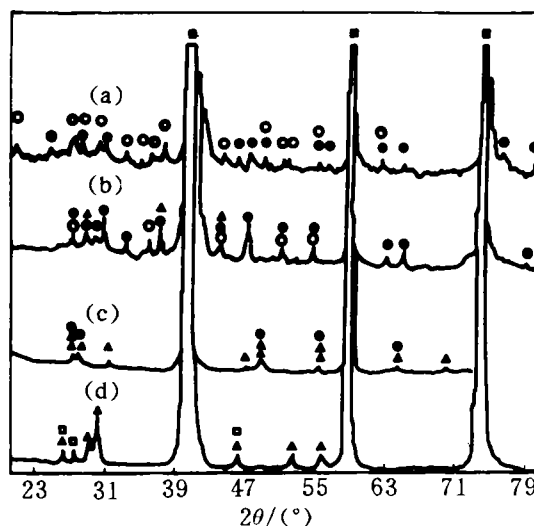


Fig. 1 X-ray spectrum of HLM powder decomposed at  $350\text{ }^\circ\text{C}$  (a),  $840\text{ }^\circ\text{C}$  (b); HLM presintered (c), and HLM electric-sintered (d)

○— $\text{La}(\text{NO}_3)_3$ ; △— $\text{La}_2\text{O}_3$ ; ▲— $\text{MoO}_3$ ; □— $\text{Mo}_4\text{O}_{11}$ ; ■—Mo; ●—oxides of La and Mo

#### 3.3 Microstructure of Annealed La-Mo Wires

Figs. 3 and 4 show the microstructures of annealed LLM and HLM wires, respectively. As seen from Fig. 3, LLM has a widening fibrous structure at  $1200\text{ }^\circ\text{C}$ , indicating the starting of recrystallization. At  $1400\sim 1500\text{ }^\circ\text{C}$ , an elongated grain is formed at areas near to surface of LLM wires, then spreads towards the centre as the annealing temperature increases. At  $1600\text{ }^\circ\text{C}$ , a complex grain structure of elongated grain and fibrous grain is ob-



Fig. 2 SEM observation of swaged bars of HLM  
(a)  $\phi 7.4$  mm; (b)  $\phi 3.0$  mm

served in LLM wires. At higher temperature, an elongated and interlocked grain has been formed in LLM wires, which is similar to that of doped tungsten. By comparison with LLM, HLM wires exhibit a different behavior of recrystallization, as shown in Fig. 4. At temperatures below  $2000^{\circ}\text{C}$ , the fibrous structure is observed in HLM wires, but this microstructure is transformed into equiaxed grains at much higher temperature ( $2200^{\circ}\text{C}$ ). Also the shape and size of  $\text{La}_2\text{O}_3$  changed during the annealing process. An elongated  $\text{La}_2\text{O}_3$  particles are observed in HLM wires annealed at temperatures below  $1600^{\circ}\text{C}$ , but these  $\text{La}_2\text{O}_3$  are breaking up at  $1600^{\circ}\text{C}$  (Fig. 4c), and turn into rows of  $\text{La}_2\text{O}_3$  particles arranged in the working direction, with particle size of  $0.3\sim 1.0\mu\text{m}$ . When the temperature increases to above  $2200^{\circ}\text{C}$ , the particle size of  $\text{La}_2\text{O}_3$  reaches  $5\sim 8\mu\text{m}$  due to the diffusion and Ostwald ripening effect (Fig. 4f).

#### 3.4 Physical and Mechanical Properties of La-Mo Wires

The dependences of resistivity, ultimate ten-

sile strength (UTS,  $\sigma_b$ ), yield strength (YS,  $\sigma_{0.2}$ ) and elongation ( $\delta$ ) of La-Mo wires and pure Mo wires on the annealing temperatures are shown in Figs. 5 and 6, respectively. As seen in Fig. 5, the resistivity remains almost unchanged for the LLM, HLM and PM during the annealing process. Compared with PM, the HLM has higher resistivity because of the addition of 6.6% volume fraction of  $\text{La}_2\text{O}_3$  which is bad conductor. But small amount of  $\text{La}_2\text{O}_3$  decreases the resistivity, which can be explained by the interaction between active La atom and O, C and N impurities or special elongated grain structure. In LLM wires, a minor La atom interacts with the O, C and N impurities, thus leading to the formation of stable rare earth compounds and decrease of the content of O, C and N impurities.

The UTS and YS of HLM wires  $200\sim 250$  MPa higher than those of PM and LLM wires, whereas the elongation of HLM is good only when annealed above the temperature  $1600^{\circ}\text{C}$ . On the other hand, LLM shows better elongation below annealing temperature  $1000^{\circ}\text{C}$ .

A different dependence of elongation on annealing temperature is found for PM, LLM and HLM wires. PM wires show maximum elongation at  $1100^{\circ}\text{C}$  due to the recovery and recrystallization of wires, then the elongation falls at higher temperatures, exhibiting recrystallization embrittlement at ambient temperature resulted from the increase of impurities at grain boundaries<sup>6</sup>. For LLM wires, a recrystallized grains are observed at  $1200^{\circ}\text{C}$ , but the grain grows very slowly due to the inhibition of secondary phases below  $1400^{\circ}\text{C}$ . When annealed at  $1400^{\circ}\text{C}$ , LLM wires show the maximum elongation, then fall down as a result of the grain growth and uneven grain structure between the sides and centre of annealed wires. Being much different with PM and LLM wires, HLM wires exhibit much higher strength but lower elongation when being annealed at a temperature below  $1600^{\circ}\text{C}$ . However, at higher temperature, the widening fiber structure and fine recrystallized grains were found in annealed HLM wires, which result in the increase of elongation of HLM wires. Another reason for increase of elongation is the decrease of dislocation pile-up at  $\text{La}_2\text{O}_3$  second phases because the  $\text{La}_2\text{O}_3$  transform from elongated shapes

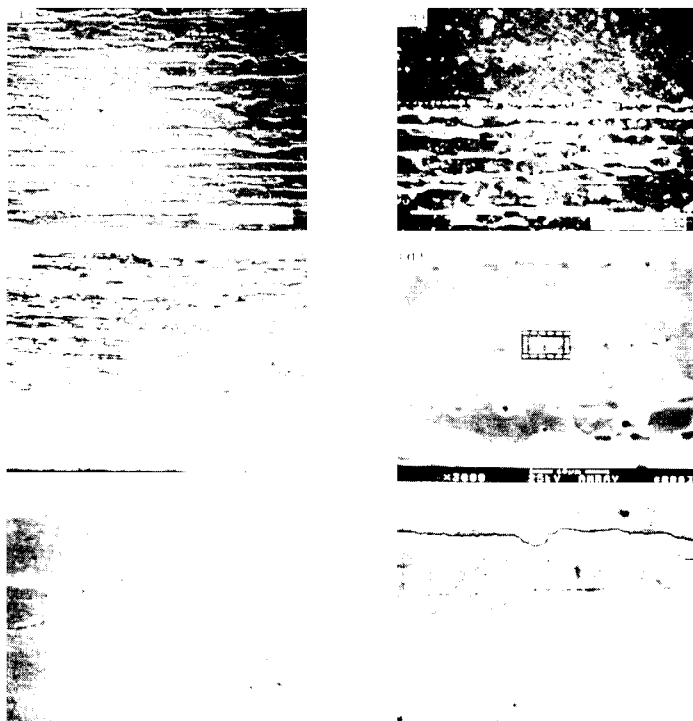


Fig. 3 Microstructures of LLM wires annealed at various temperatures

to spherical shapes when HLM wires annealed at temperatures above 1600 °C.

3.5 High-Temperature Creep-Resistant Property of La-Mo Wires

The creep properties of PM and La-Mo wires were tested according to "V" type non-sag method. And the results were listed in Table 2, which indicated the creep strength of Mo wires is greatly improved by doping with small amount of La<sub>2</sub>O<sub>3</sub>, but creep strength degraded with La<sub>2</sub>O<sub>3</sub> content increas-

ing to 4.0 wt.-%. This can be explained by the Herring-Nabarro equation<sup>7</sup>:

$$\dot{\epsilon} = ADG\Omega / (KTd^2) \tag{1}$$

Table 2 Creep properties of PM, LLM and HLM wires

Creep	PM	LLM	HLM
$\dot{\epsilon}$ /S/mm	15.7	7.0	16.0

Under the condition of diffusion of grain boundary, creep rate is given by Coble<sup>8</sup>:

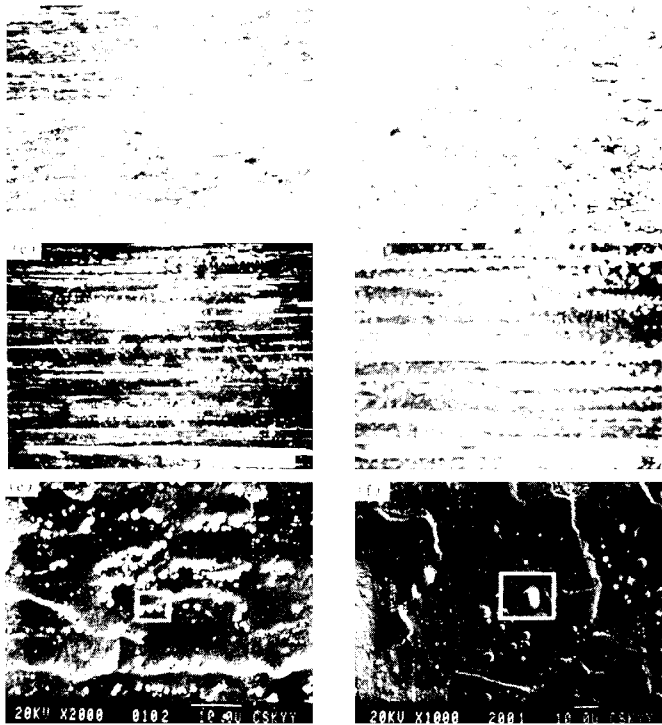


Fig. 4 Microstructure and changes of La<sub>2</sub>O<sub>3</sub> during annealing process

$\dot{\epsilon} = A'D'\sigma\Omega/(KTd^2)$  (2)  
 where  $\sigma$ —stress;  $D$ —diffusion coefficient;  $D'$ —grain boundary diffusion coefficient;  $d$ —grain size;  $\Omega$ —atom volume;  $T$ —Kelven temperature;  $K$ —Boltzman constant;  $A, A'$ —constants.

According to equations (1) and (2), the high-temperature creep resistant properties of La-Mo wires are determined by the grain sizes. Therefore, the LLM wires show excellent creep resistant property due to the larger elongated recrystallized grain structure, whereas fine equiaxed recrystal-

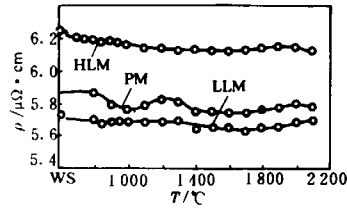


Fig. 5 Dependence of resistivity of La-Mo wires on annealing temperatures

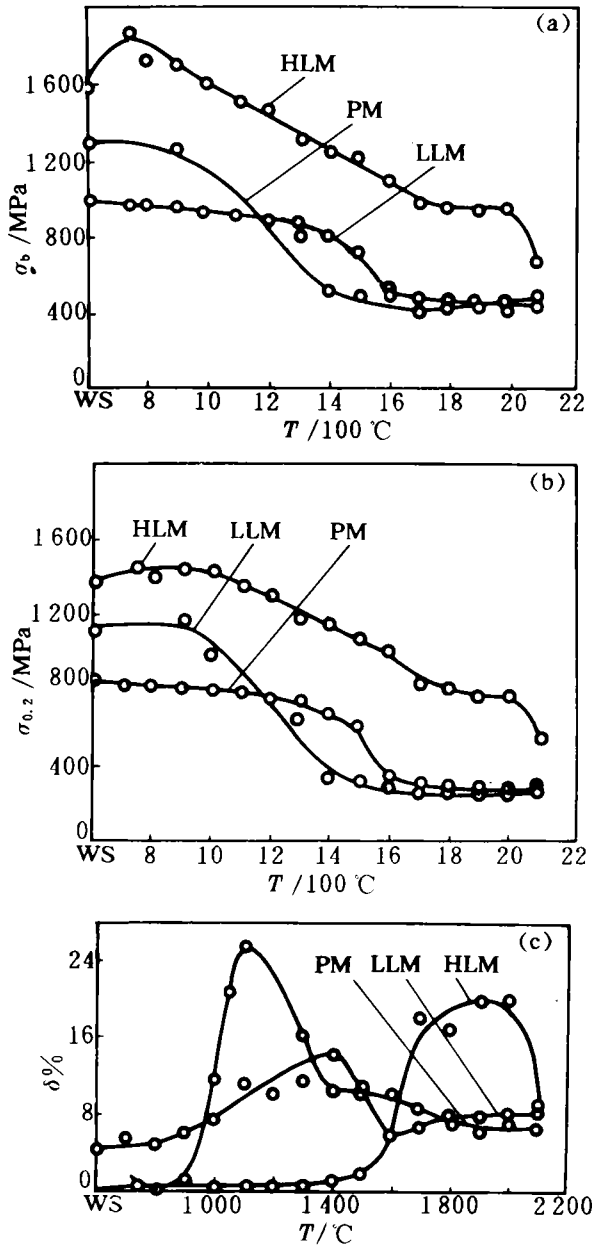


Fig. 6 Variation of strength and elongation with annealing temperatures  
(a)—UTS~T; (b)—YS~T; (c)— $\delta\%$ ~T

lized grains were formed in HLM wires, thus it exhibits poor creep-resistant property.

### 3.6 Thermionic Electron Emission Property

The electron tubes equipped with this new La-Mo cathode material have been designed and tested. The results indicate that the electron emissive capacity of La-Mo cathode under lower operating voltage reaches or surpasses that of Th-W cathode, as shown in Fig. 7. But current of the La-Mo tube attenuates with time, whereas the current of Th-W tube is very stable. The capacity and stability of La-Mo electron tube is possibly related to the reduction, diffusion and evaporation of  $\text{La}_2\text{O}_3$ . The detailed mechanism is under investigation.

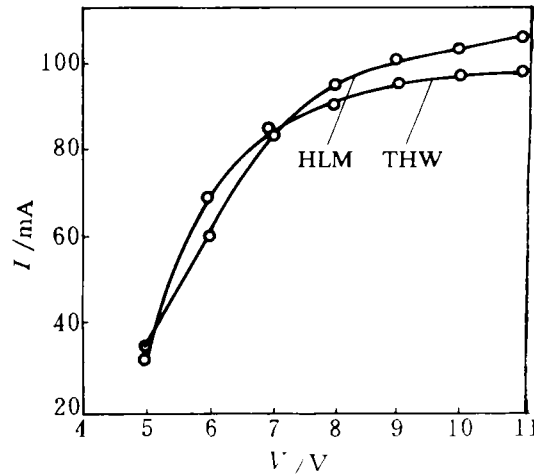


Fig. 7 Comparison of thermionic electron emissive capacity of La-Mo cathode with Th-W cathode

## 4 CONCLUSIONS

(1) The particle size of Mo powders and the grain of Mo ingot were refined for addition of  $\text{La}_2\text{O}_3$ . Meanwhile, the La-Mo wires show higher recrystallization temperature than PM wires.

(2) The La-Mo wires exhibit a very different recrystallization behavior, physical properties and mechanical properties due to the addition of  $\text{La}_2\text{O}_3$ . La exists mainly in the form of  $\text{La}_2\text{O}_3$  along the working direction.  $\text{La}_2\text{O}_3$  breaks up into particles at 1600°C and distributes along the grain boundaries at elevated temperature.

(3) The high-temperature creep-resistant properties of Mo wires were greatly improved by doping  
(To page 66)

great advances; The completely empirical  $W_1(r)$  potential related to electronic structure of crystals; The  $W_1(r)$  potential with two atoms interaction has been developed into  $W_z(r)$  potential with many-atoms interaction; The relationships of parameters in  $W_z(r)$  potential, various elastic moduli and thermal expansion coefficient as a function of temperature with microquantities have been derived, so the natures of these parameters and properties of crystals have been more clear.

(3) The relationships of parameters  $n_m$  and  $\alpha_m$  in  $W_m(r)$  potential with parameters  $m_z$  and  $n_z$  in  $W_z(r)$  potential have been established:

$$\begin{cases} n_m = n_z / (n_z - 1) \\ \alpha_m = m_z (r - r_0) \ln(r - r_0) / n_z \end{cases}$$

when  $W_m(r)$  potential is used to study interaction of atoms of crystals, the parameter  $\alpha_m$  generally is a constant, but  $(r - r_0) \ln(r - r_0)$  is not constant, so  $W_m(r)$  and  $W_z(r)$  potentials can not transfer each other, and can not be able to have identical po-

tential curve.

## REFERENCES

- 1 Lennard-Jones, J E. *Physica*, 1937, (10): 941.
  - 2 Milstein, F. *J Appl Phys.* 1937, (44): 3825.
  - 3 Xie, Y Q. *Science in China, Series A*, 1993, (1): 90.
  - 4 Xie, Y Q *et al.* *Transactions of NFsoc*, 1992, (2): 56.
  - 5 Xie, Y Q *et al.* *Science in China, series A*, 1993, (4): 487.
  - 6 Xie, Y Q *et al.* *Science in China, series A*, 1993, (4): 495.
  - 7 Xie, Y Q; Ma, L Y. *Journal of Central-South Institute of Mining and Metallurgy*, 1985, (1): 1.
  - 8 Xie, Y Q *et al.* *Chinese Science Bulletin*, 1992, (16): 1529.
  - 9 Gray, E E. *American Institute of Physics Handbook*. 3rd edition. New York, Toronto, London: McGraw-Hill Book Company, Inc. 1972. 4-119.
- 
- (From page 62)
- of small amount of  $\text{La}_2\text{O}_3$ , whereas the La-Mo wires doped with higher content of  $\text{La}_2\text{O}_3$  show very good toughness at room temperature when annealed at higher temperatures and have excellent thermionic electron emissive capacity.
- ## REFERENCES
- 1 Lee, K S. *Journal of the Less-common Metals*, 1984, 99: 215-244.
  - 2 Endo, M. In: 12th Inter Plansee Seminal, 1989, 1. 37-52.
  - 3 Eck, R. In: 12th Inter Plansee Seminal, 1989, 1. 483-491.
  - 4 Zhou, Meiling *et al.* *Materials Science and Engineering of Rare Metals*, 1989, (6): 11-15.
  - 5 Bachmann, R; Busbau, C; Gessinger G. US 4083811. 1978.
  - 6 Zuo, Tiejong *et al.* *J of Central-South Institute of Mining and Metallurgy*, 1982, (1): 47-53.
  - 7 Herring, C. *J Appl Phys*, 1950, 21: 437.
  - 8 Coble, B L. *J Appl Phys*, 1963, 34: 1979.
  - 9 zhou, M; Cheng, Z; zhang, J; Li, J; Zuo, T. In: 13th Inter Plansee Seminal, 1993, 1: RM70.